Uncoupled achromatic condition of a dog-leg system with the presence of RF cavities*

GENG Hui-Ping(耿会平)[1)] GUO Zhen(郭臻)

Institute of High Energy Physics, Chinese Academy of Sciences, Beijing 100049, China

Abstract: To merge the beam from either of the two injectors to the main linac, a dog-leg system will be employed in the second Medium Energy Beam Transport (MEBT2) line of the China ADS driving accelerator. The achromatic condition has to be guaranteed to avoid beam center excursion against energy jitter. RF cavities were found to be indispensable to control the bunch length growth in the dog-leg system of MEBT2. The full uncoupling between transverse and longitudinal plane is desired to minimize the growth of projected rms emittances. The uncoupled achromatic condition of this dogleg system with the presence of RF bunching cavities will be deduced using the transfer matrices method. It is found that, to fulfill the uncoupling condition, the distance between the bunching cavities is uniquely determined by the maximum energy gain of the RF cavities. The theoretical analysis is verified by the simulation code TraceWin. The space charge effect on the uncoupled achromatic condition and the beam emittance growth will also be discussed.

Key words: dog-leg system, achromatic, coupling, transfer matrix, medium energy

PACS: 41.75.-i, 41.85.-p, 29.27.-a **DOI:** 10.1088/1674-1137/38/6/067001

1 Introduction

The C-ADS accelerator is a CW proton linac that uses superconducting acceleration structures, except for the RFQs [1]. To ensure the high reliability of the accelerator at low energy, two parallel injectors are to be designed, whereby one will be a 'hot spare' of the other. The second Medium Energy Beam Transport (MEBT2) is to transport and match the beam from either of the two injectors to the main linac. A dog-leg system will be employed in the MEBT2 line of the China ADS accelerator.

An achromatic condition has to be guaranteed to avoid beam center excursion against energy jitter. The latest design of MEBT2 [2] shows that RF cavities are indispensable to control the bunch length growth and emittance growth in the dog-leg system of MEBT2. With the presence of RF cavities in a bending section, there will be coupling between transverse and longitudinal planes, which may cause extra emittance growth. The full uncoupling between transverse and longitudinal planes is desired to minimize the growth of projected rms emittance.

In this paper, the uncoupled achromatic condition of a dogleg system with the presence of RF bunching cavities will be deduced using the transfer matrices method. The analytical result will be checked by simulations carried out with the code TraceWin [3]. The space charge effect will also be briefly discussed.

2 Theoretical analysis

The typical layout of a dog-leg section with the presence of two bunching cavities is shown in Fig. 1. The two bending magnets bend the beam by the same angle but to opposite directions, the red dot represents the RF cavities and the dotted rectangle represents any combination of quadrupoles and drifts.

The transfer matrix of a bending magnet that bends the beam to the right can be written as,

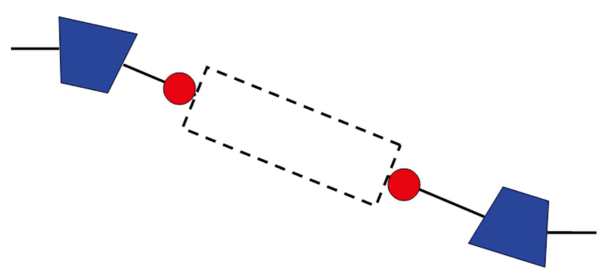

Fig. 1. A typical layout of a dog-leg section with RF cavities.

Received 4 July 2013

∗ Supported by National Natural Science Foundation of China (10875099, 91126003) and China ADS Project (XDA03020000)

1) E-mail: genghp@mail.ihep.ac.cn

$$M_{b_+}=\begin{pmatrix} b_{11} & b_{12} & 0 & 0 & 0 & b_{16} \\ b_{21} & b_{22} & 0 & 0 & 0 & b_{26} \\ 0 & 0 & 1 & b_{34} & 0 & 0 \\ 0 & 0 & 0 & 1 & 0 & 0 \\ -b_{26} & -b_{16} & 0 & 0 & 1 & b_{56} \\ 0 & 0 & 0 & 0 & 0 & 1 \end{pmatrix}, \tag{1}$$

where b_{ij} denotes the element of the transfer matrix in the ith row and jth column. b_{ij} is normally a function of the bending radius and bending angle.

A bunching cavity can be replaced by a RF gap for simplicity. Assuming the beam energy does not change much after passing through the gap, the transfer matrix of the beam can be written as,

$$M_{\rm gap}=\begin{pmatrix} 1 & 0 & 0 & 0 & 0 & 0 \\ 1/f_x & 1 & 0 & 0 & 0 & 0 \\ 0 & 0 & 1 & 0 & 0 & 0 \\ 0 & 0 & 1/f_y & 1 & 0 & 0 \\ 0 & 0 & 0 & 0 & 1 & 0 \\ 0 & 0 & 0 & 0 & -1/f_z & 1 \end{pmatrix}, \tag{2}$$

where

$$f_x=f_y=-\frac{m_0c^2}{\pi q}\frac{\beta^3\gamma^3\lambda}{E_0TL\sin\phi_{\rm s}}, \tag{3}$$

and

$$f_z=-\beta\gamma\cdot\frac{m_0c^2}{2\pi q}\frac{\beta^2\lambda\sin\phi_{\rm s}}{E_0TL}, \tag{4}$$

where m_0 is the rest mass of the particle, q is the charge of the particle, c is the velocity of light, γ and β are the Lorentz factor and normalized velocity of the particle, λ is the wavelength of the RF, E_0TL is the maximum energy gain or effective voltage of the cavity, and $\phi_{\rm s}$ is the synchrotron phase.

The transfer matrix of a system, which is a combination of quadrupoles and drifts, can be represented by

$$M_{\rm fodo}=\begin{pmatrix} R_{11} & R_{12} & 0 & 0 & 0 & 0 \\ R_{21} & R_{22} & 0 & 0 & 0 & 0 \\ 0 & 0 & R_{33} & R_{34} & 0 & 0 \\ 0 & 0 & R_{43} & R_{44} & 0 & 0 \\ 0 & 0 & 0 & 0 & 1 & R_{56} \\ 0 & 0 & 0 & 0 & 0 & 1 \end{pmatrix}. \tag{5}$$

Here R_{ij} is a function of the quadrupoles strengths and drifts lengths. Assuming the total length of the fodo system is L_d, then $R_{56}=L_d/\gamma^2$.

The transfer matrix of a drift space with a length of d at low energy can be written as

$$M_d=\begin{pmatrix} 1 & d & 0 & 0 & 0 & 0 \\ 0 & 1 & 0 & 0 & 0 & 0 \\ 0 & 0 & 1 & d & 0 & 0 \\ 0 & 0 & 0 & 1 & 0 & 0 \\ 0 & 0 & 0 & 0 & 1 & d/\gamma^2 \\ 0 & 0 & 0 & 0 & 0 & 1 \end{pmatrix}. \tag{6}$$

The whole dog-leg section can be described by matrix multiplication:

$$M=M_{b-}\cdot M_D\cdot M_{\rm gap2}\cdot M_{\rm fodo}\cdot M_{\rm gap1}\cdot M_d\cdot M_{b_+}, \tag{7}$$

where M_{b-} and M_{b_+} are the transfer matrices of bending magnets which bend the beam to the left and right, M_D and M_d are the transfer matrices of drifts with length of D and d, $M_{\rm gap1}$ and $M_{\rm gap2}$ are the transfer matrices of RF gaps with longitudinal focal length of f_z and F_z, and $M_{\rm fodo}$ is the transfer matrix of a section composed of quadrupoles and drifts.

Assuming that the two bending magnets are identical to each other, then M_{b-} can be expressed as,

$$M_{b_-}=\begin{pmatrix} b_{11} & b_{12} & 0 & 0 & 0 & -b_{16} \\ b_{21} & b_{22} & 0 & 0 & 0 & -b_{26} \\ 0 & 0 & 1 & b_{34} & 0 & 0 \\ 0 & 0 & 0 & 1 & 0 & 0 \\ b_{26} & b_{16} & 0 & 0 & 1 & b_{56} \\ 0 & 0 & 0 & 0 & 0 & 1 \end{pmatrix}. \tag{8}$$

After some tedious but straight forward matrix multiplication, we have:

$$M_{15}=M_{62}=-b_{16}\cdot[-(1-R_{56}/F_z)/f_z-1/F_z], \tag{9}$$

and also,

$$M_{25}=M_{61}=-b_{26}\cdot[-(1-R_{56}/F_z)/f_z-1/F_z], \tag{10}$$

where M_{ij} is the element of matrix M in the ith row and jth column.

To decouple the transverse from the longitudinal plane, it is required that

$$-(1-R_{56}/F_z)/f_z-1/F_z=0, \tag{11}$$

or

$$R_{56}=f_z+F_z. \tag{12}$$

We can see from Eq. (12) that R_{56}, or the distance between the two RF cavities, has a minimum when the two RF cavities have the same focusing length.

Given $f_z=F_z$, Eq. (12) can be written as,

$$R_{56}=2f_z. \tag{13}$$

Assume that the synchronous phase of the two RF cavities are both $-90°$ to maximize the bunching effect, Eq. (13) can be written as,

$$L_d=\frac{\lambda}{\pi}\cdot\frac{m_0c^2}{q}\cdot\frac{\beta^3\gamma^3}{E_0TL}. \quad (14)$$

This relation in Eq. (14) states that the distance of the two RF cavities is uniquely determined by their effective voltage to be able to decouple the transverse from longitudinal. For high energy electron beams, $\gamma\gg1$ gives $L_d\gg1$, which implies that no longitudinal bunching will be necessary when a high energy electron beam is transporting a bending section, which agrees with our common knowledge.

The other coupling terms (e.g. M_{16} and M_{26}) have strong dependence on the transverse focusing strengths or elements of $M_{\rm fodo}$. The full decoupling of transverse and longitudinal can be achieved by adjusting the quadrupole strengths with the help of simulation codes, such as TraceWin.

It is worth mentioning that a similar analysis can be carried out for a bending section with the presence of only one bunching cavity. It can be easily found that the uncoupled achromatic condition could not be fulfilled; thus, at least two bunching cavities will be needed for such a dog-leg system.

3 Simulation result

The input beam parameters are assumed to be the same as the ones for C-ADS MEBT2, except that the beam current is set to zero in order to eliminate space charge effect. The detailed beam parameters used for simulations are summarized in Table 1.

Table 1. Input beam parameters used for simulation of the C-ADS like dog-leg section.

parameter	value
current/mA	0
beam energy/MeV	10.0
ϵ_x/(mm·mrad)	0.21
ϵ_y/(mm·mrad)	0.20
ϵ_z/(mm·mrad)	0.16
α_x	−1.44
β_x/(πmm·mrad)	2.70
α_y	−1.42
β_y/(πmm·mrad)	2.68
α_z	−0.31
β_z/(πmm·mrad)	0.99

We check the validity of Eq. (14) with an C-ADS MEBT2 like dog-leg section. The dog-leg is composed of two bending magnets, two sets of triplets and two bunching cavities. The layout of the dog-leg section is shown in Fig. 2.

Two bending magnets are used in the dog-leg section and the two bending magnets are identical, with the exception that the first one bends the beam to the right while the second one bends the beam to the left. The bending radius is 0.936 m and the bending angle is 20°.

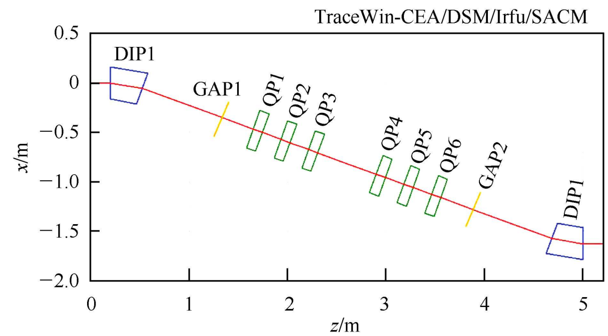

Fig. 2. The layout of a C-ADS MEBT2 like dog-leg section.

Table 2. Parameters list for the C-ADS like dog-leg section.

element	length/mm	strength/(T/m)(kV)
D1	200	—
B	326.8	—
D2	800	—
GAP1	0	300
D2	400	—
Q1	100	−7.2
D3	200	—
Q2	100	9.1
D4	200	—
Q3	100	−2.8
D5	690	—
Q4	100	−2.8
D6	200	—
Q5	100	9.8
D7	200	—
Q6	100	−8.5
D8	400	—
GAP2	0	300
D9	800	—
B	326.8	—
D10	200	—

The bunching cavities are represented by RF gaps that have synchronous phases of −90°. The maximum energy gain of the RF gaps are assumed to be 300 kV, which is about twice the feasibility of normal conducting cavities working at continuous wave mode at a beam energy of 10 MeV. The distance between the two RF cavities is calculated by Eq. (14) and has been set up accordingly. The strength of the quadrupoles has been adjusted to fulfill the achromatic condition, namely $R_{16}=R_{26}=0$. The detailed parameters list can be found in Table 2.

The resulted transfer matrix elements M_{15}, M_{62} and M_{25}, M_{61} are shown in Fig. 3 and Fig. 4, respectively.

We can see from Fig. 3 that M_{61} and M_{62} are produced by the coupling of transverse to longitudinal when passing through the RF gap at a dispersive section. They can be eliminated after passing through the second gap by properly choosing the distance between the two RF gaps. M_{15} and M_{25} maintains zero until the second bending magnet. The final value of M_{15} and M_{25} at the exit of the second bending magnet can be suppressed by properly choosing the distance between the two RF gaps, as shown in Eq. (9) and Eq. (10). It should be reminded that these properties of M_{61}, M_{62}, M_{15} and M_{25} are not subject to the strength of the quadrupoles along the bending section.

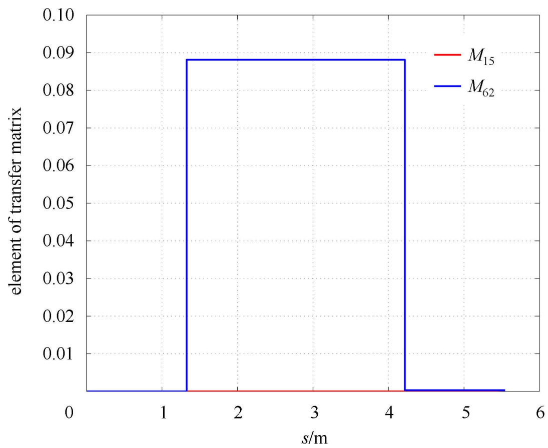

Fig. 3. The M_{15} and M_{62} elements of beam transfer matrix M. These elements are predicted to be zero by Eq. (9).

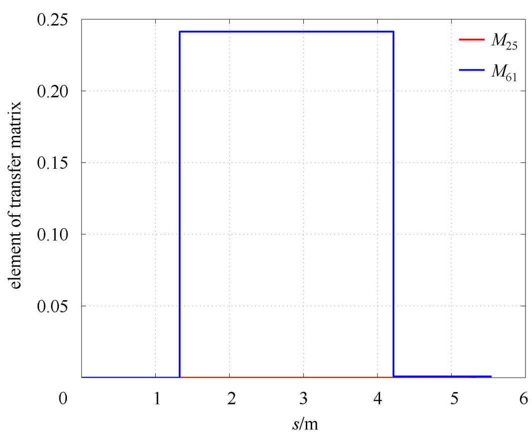

Fig. 4. The M_{25} and M_{61} elements of beam transfer matrix M. These elements are predicted to be zero by Eq. (10).

The dispersive terms M_{16} and M_{26} are strongly dependent on the setup of the quadrupoles strengths. The achromatic condition can be fulfilled by properly adjusting the strengths of the six quadrupoles. The results are shown in Fig. 5 and Fig. 6. We can see that both M_{16}, M_{26} and M_{51}, M_{52} and returns to zero after exiting the second bend.

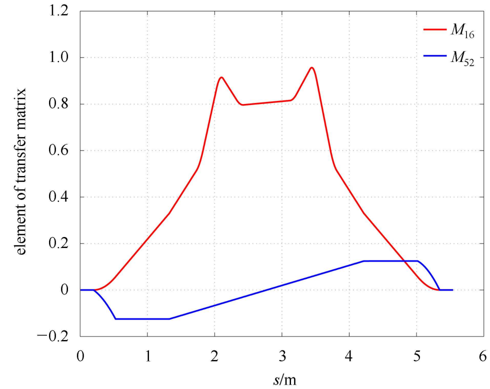

Fig. 5. The M_{16} and M_{51} elements of beam transfer matrix. The strengths of quarupoles are adjusted to have $M_{16}=M_{26}=0$.

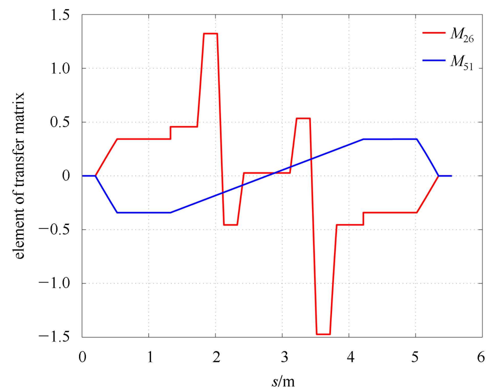

Fig. 6. The M_{26} and M_{51} elements of beam transfer matrix. The strengths of quarupoles are adjusted to have $M_{16}=M_{26}=0$.

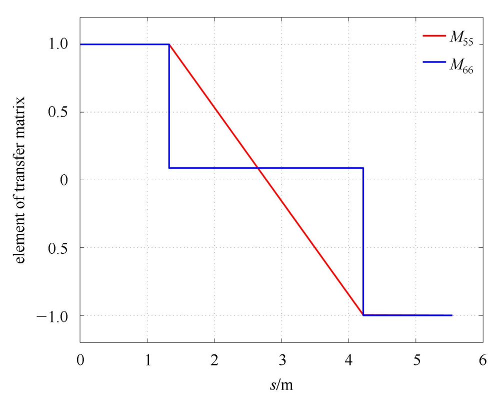

Fig. 7. The M_{55} and M_{66} elements of beam transfer matrix. $M_{55} = M_{66} = -1$ or the reversal of the longitudinal phase space is guaranteed by Eq. (13).

The relationship of Eq. (13) also guarantees another important feature of the dog-leg system, which is the reversal of the longitudinal phase space, namely $M_{55}=M_{66}=-1$. The reversal of the longitudinal phase space also explains why the dog-leg system is symmetric instead of anti-symmetric achromatic. The $M_{55}=M_{66}=-1$ of the dog-leg system is shown in Fig. 7.

Since the whole system is fully uncoupled, as can be seen in Fig. 3 to Fig. 6, we would expect no growth of projected rms emittance in all three planes. The resulting projected emittance of the dog-leg system is shown in Fig. 8. It is easy to see that the rms emittances remain the same after passing through the whole system. The growth of projected emittance in the middle of the bending section is caused by the coupling of transverse and longitudinal planes.

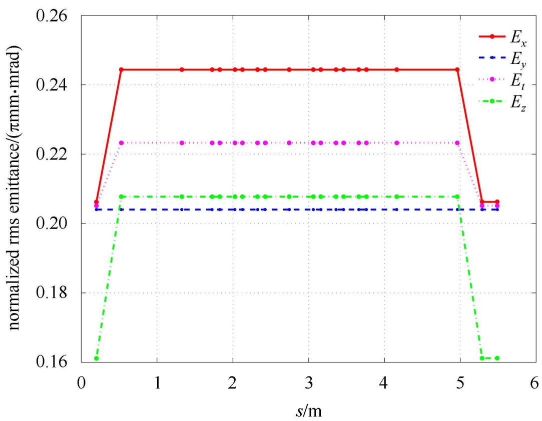

Fig. 8. The evolution of projected rms emittances in x,y, 4D transverse and z planes.

4 Space charge effect

The inclusion of a space charge effect will break the simple law of Eq. (14) to fully decouple transverse from longitudinal. The distortion of uncoupling condition from the space charge effect will lead to the growth of the projected emittance. It has been proved that decoupling, with the exclusion of the space charge effect, is an essential way to minimize the beam emittance growth [4]. We simulate the effect of space charge effect on the emittance growth of the dog-leg section that is described in the previous section. Gaussian distributions in all three planes are assumed. Ten thousand macro particles are used in the simulation. We keep the input beam parameter the same and gradually increase beam current from 0 mA to 40 mA. The change of projected rms emittances at the end of the dog-leg section in x, y and z planes as the beam current increases are shown in Fig. 9.

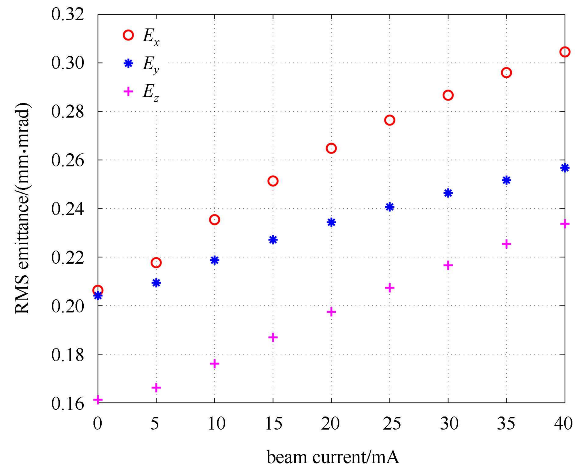

Fig. 9. The change of projected rms emittances in x, y and z planes as the beam current increases from 0 mA to 40 mA.

We can see that the projected emittance grows in all three planes as the beam current increases. The growth rate of the emittances in x and z planes are consistent with each other due to the residual coupling caused by the space charge effect. The emittance in y plane grows slower than in the other two planes since the coupling is weaker with the absence of bending in the y plane.

5 Conclusions

The uncoupled achromatic condition has been analyzed for a C-ADS like dog-leg system with the presence of RF cavities. Theoretical analysis has shown that at least two cavities are required to decouple transverse from longitudinal planes. An explicit formula was given to determine the distance between two cavities in order to realize the uncoupling. It is shown that the distance between two cavities is inversely proportional to the maximum energy gain in each cavity. Proof of principle simulations were done with the code TraceWin. The simulation results agree well with the theoretical analysis.

The formula deduced in this paper can help determine the element layout when designing a dog-leg system that has to incorporate RF cavities.

Huiping Geng would like to thank Dr. Xiaoyu Wu and Dr. P.A. Phi Nghiem for their useful discussions.

References

1 TANG J Y et al. Conceptual Physics Design on the C-ADS Accelerator. IHEP-CADS-Report/2011-1E
2 GENG H, TANG J et al. High Power Laser and Particle Beams, 2013, **25**(3): 1005 (in Chinese)
3 http://irfu.cea.fr/Sacm/logiciels/index3.php
4 GUO Zhen. C-ADS MEBT2 Physics Design (Master Thesis). Beijing: Institute of High Energy Physics, CAS, 2013 (in Chinese)